New Journal of Physics
The open-access journal for physics

# Aharonov–Bohm phase shifts induced by laser pulses

**B Barwick**[1] **and H Batelaan**[2,3]

[1] Arthur Amos Noyes Laboratory of Chemical Physics,
California Institute of Technology, Mail Code 127-72,
1200 East California Boulevard, Pasadena, CA 91125, USA
[2] Department of Physics and Astronomy, University of Nebraska–Lincoln,
116 Brace Laboratory, PO Box 880111, Lincoln, NE 68588-0111, USA
E-mail: hbatelaan2@unl.edu

*New Journal of Physics* **10** (2008) 083036 (9pp)
Received 27 May 2008
Published 26 August 2008
Online at http://www.njp.org/
doi:10.1088/1367-2630/10/8/083036

**Abstract.** An experimentally accessible scalar Aharonov–Bohm (AB)-effect is proposed using a ponderomotive potential induced by a pulsed laser. This ponderomotive AB (PAB)-effect is unique in that the time-averaged description is classified as type-I, whereas the underlying time-dependent theory is classified as type-II. Not only is the PAB-effect of fundamental interest, it may also be used to characterize ultrashort electron pulses ($<100$ fs), using low power femtosecond lasers, which is important for ultrafast electron diffraction and microscopy.

It is well known that in quantum mechanics both electric and magnetic fields can affect systems non-locally. Aharonov and Bohm (AB) brought this behaviour to the forefront by proposing two experiments. Nonzero scalar and vector potentials were shown to cause phase shifts in an electron interferometer, even though no electric or magnetic fields are present at the location of the electron [1]. While the magnetic AB-effect has been observed for electrons [2, 3], the electric AB-effect, as originally proposed, has not. Lee *et al* [4] performed an experiment using neutrons that shows an effect that is similar in nature to the electric AB-effect. However, because this experiment requires the neutron to be in the presence of local electromagnetic fields, the effect is a type-II effect. Type-II effects are defined as those that arise through local interactions with fields, yet also end up with wave packets accumulating a non-local phase shift, *identical* in measurable consequences to type-I AB-effects [5]. Matteucci and Pozzi [6]

[3] Author to whom any correspondence should be addressed.

performed diffractive experiments to test scalar AB-effects, however, the effect resulted in classical deflections, and hence cannot be considered an AB-effect.

In this paper, we demonstrate that the use of a pulsed ponderomotive interaction instead of the usual pulsed electric potential satisfies all criteria of an AB-effect. This PAB-effect requires a laser pulse to be crossed with one of the arms of an electron interferometer. Four descriptions (a, b, c and d) are provided for this physical scenario. (a) The ponderomotive potential can be substituted for the electric potential in the expression for the electric AB-effect. (b) To justify this substitution a cycle-averaged path integral formulation is provided. These two approaches are useful as they expound the similarity to the electric AB-effect and provide a simple calculation of the correct PAB-phase shift.

A more complete description (c) that includes the time-dependent interaction between the electron and light, for which the laser electric and magnetic fields are present locally, yields an identical answer, justifies the cycle-averaged approaches and shows that the effect must be classified as type-II. The discussed physical scenario satisfies the defining criteria of all AB-effects, in the sense that no classical time lag or deflection is induced, local effects of the interaction are masked by the quantum uncertainties of the system, and the phase shift is dispersionless. Finally, (d) a numerical simulation with realistic fields and realistic electron interferometer parameters fully supports the above claims.

While the PAB-effect complements our physical understanding of the AB-effect, it may also prove useful for the characterization of ultrashort electron pulses. Ultrashort electron pulses of 10 fs are now considered to be an ultimate goal for such applications as ultrafast electron microscopy and diffraction [7]–[11]. The reason is that most chemical processes occur at a timescale of 10 fs to 1 ps [12]. However, at present only indirect methods have been used to infer the electron pulse durations on the sub-100 fs scale [7, 8]. The ability to directly measure ultrashort electron pulses is currently limited to streak camera methods [13], or direct electron bunch sampling with intense femtosecond laser pulses [14, 15]. These methods have drawbacks due to their temporal resolution (streak cameras) or their requirements for high-intensity femtosecond lasers ($\sim 10^{17}\,\mathrm{W\,cm^{-2}}$) [14, 15]. While other methods of pulse characterization have been proposed (see [16, 17]), we show that by using the phase sensitivity of an electron interferometer the laser intensity necessary to directly sample an ultrashort electron pulse is reduced to $\sim 10^{13}\,\mathrm{W\,cm^{-2}}$.

The electric AB-effect arises from the fact that potentials, such as the electric potential can give rise to quantum mechanical phase shifts. The electric AB-phase shift accumulated by an electron that travels through a metallic tube is

$$\Delta\phi_{\mathrm{AB}} = 1/\hbar \int e\Phi(t)\,\mathrm{d}t, \tag{1}$$

where the time-dependent electric potential of the tube is represented by $\Phi(t)$ and the integration is performed over the voltage pulse duration [1]. This phase shift does not itself give rise to any locally measurable changes, but can be measured by using an electron interferometer. The setup needed to measure this phase shift is depicted in figure 1(a), and involves the separation of an electron wave packet into two parts, with the two electron paths passing through spatially separate metallic tubes. The electron interferometer must be pulsed so that when the two electron packets are fully contained in their separate metallic cylinders, the voltage on one (or both) of the tubes can be raised or lowered. The time integral of the electric potential (equation (1)) on the tubes can thus be measured as a phase shift after the two electron paths are

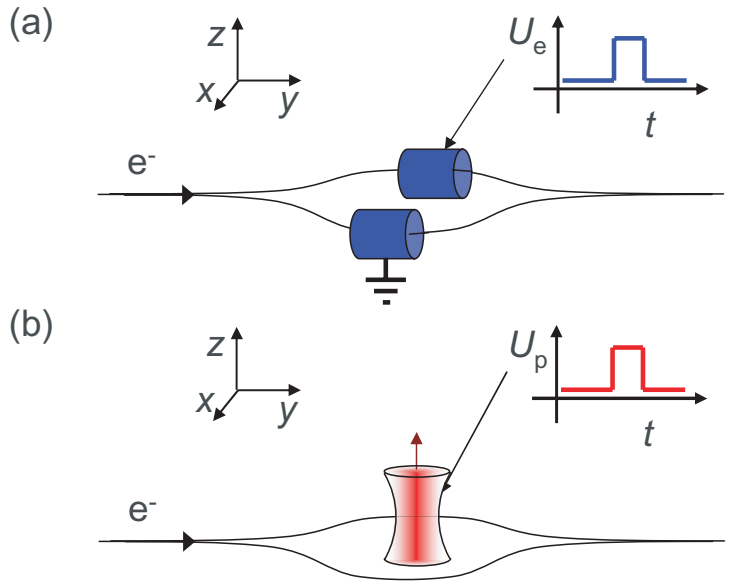


**Figure 1.** Comparison of electric AB-effect with the proposed ponderomotive AB-effect. A physical system for the realization of the electric AB-effect is given in (a), where $U_e$ is the electric potential due to a charged metallic tube (blue). A physical system for the realization of the PAB-effect is given in (b), where $U_p$ is the ponderomotive potential due to a laser-field (red).

recombined and allowed to interfere. This physical system was discussed in detail in Aharonov and Bohm's original paper [1].

The electric AB effect cannot be explained by classical mechanics due to the absence of any electric or magnetic fields (in the vicinity of the electron wave) and hence the absence of forces. To date this effect has not been observed. There are two main experimental problems that have made the observation of this effect difficult. The first is that a wide-angle electron interferometer is needed. At present there are only two possible ways to construct a separate arm electron interferometer. The first uses a combination of a field emission tip electron source with bi-prism wires [18], a technique which has been used successfully for many experiments. Recently, we realized a Mach–Zehnder interferometer with three metallic coated nanofabricated gratings [19]. For such interferometers, the arm separation is small (micrometres) hampering the placement of metallic tubes. The second experimental difficulty that arises is related to the required rapid switching of the tube voltages. This high frequency switching of the voltages on the tubes will cause transient fields inside the tube. These transient fields can mask the electric AB phase shift [20]. While the experimental difficulties preclude the observation of the electric AB-effect using current technology, the parameters of the proposed PAB-experiment (figure 1(b)) are accessible with existing lasers and electron interferometers.

(a) An electron in a laser pulse experiences the cycle-averaged ponderomotive potential [21],

$$U_{\mathrm{P}}(\vec{r},t)=\frac{\mathrm{e}\vec{A}_0^2(\vec{r},t)}{4m_{\mathrm{e}}}=\frac{e^2\lambda^2}{8\pi^2 m_{\mathrm{e}}\varepsilon_0 c^3}I(\vec{r},t), \tag{2}$$

where $I(\mathbf{r},t)$ is the intensity of the laser pulse, $\vec{A}_0$ is the peak vector potential and $\lambda$ is the optical wavelength. To make sure that the electron does not travel through gradients in the

ponderomotive potential, the requirement, $w_0/v_e \gg t_{pulse}$, where $w_0$ is the laser waist, $v_e$ is the electron speed and $t_{pulse}$ is the duration of the laser pulse, needs to be satisfied. This ensures that the distance that the electron travels is much shorter than the laser waist size during the time that the laser pulse is on. Substituting the electric potential in equation (1) by the ponderomotive potential gives the PAB-phase shift,

$$\Delta\phi_P(\mathbf{r}, t) = 1/\hbar \int U_P(\mathbf{r}, t)\, dt, \tag{3}$$

where the integration interval exceeds the laser pulse duration. A similar phase shift was proposed by Dawson and Fried [22]. However, in that paper the laser is not pulsed and consequently the relation to AB-type effects was not discussed. Hsiang and Ford [23] calculate a loss of contrast due to a fluctuating AB-phase shift for an electron travelling through a plane electromagnetic wave. The fluctuation is attributed to a random electron birth time with respect to the electromagnetic field oscillation. For our thought experiment the laser is not present at the electron source, and only present in one arm. No loss of contrast is a consequence. Evans [24] proposed the optical AB(OAB)-effect as a test of a modified electromagnetics theory, the so-called '$B^{(3)}$-theory'. The OAB-effect is thought to occur for circularly polarized light only, passing between the arms of an electron interferometer, and is purely of a type-I character.

The ponderomotive phase shift (equation (3)) accumulated by an electron wave for a laser period is

$$\Delta\phi_p = \pi e^2 E_0^2 / 2 m_e \hbar \omega^3, \tag{4}$$

where $\omega$ is the laser angular frequency and $E_0$ is the peak electric field of the laser.

(b) To justify the replacement of the electric potential with the ponderomotive potential a path integral argument can be given. The phase shift is $\phi = 1/\hbar \int L dt$, where $L = 1/2 m_e \dot{\vec{x}}^2 + e\vec{A}\cdot\dot{\vec{x}} - e\Phi$ [25] is the Lagrangian. For a laser field ($\Phi = 0$) the phase shift is $\phi = 1/\hbar \int \frac{1}{2} m \dot{\vec{x}}^2\, dt + e/\hbar \int \vec{A}\cdot\dot{\vec{x}}\, dt$. At non-relativistic laser intensities the equation of motion for an electron in a plane travelling wave is well approximated by $m\ddot{\vec{x}} = \vec{F} = -e\, d\vec{A}/dt$, yielding a momentum $m\dot{\vec{x}} = -e\vec{A} + m\dot{\vec{x}}_0$, where $\dot{\vec{x}}_0$ is the incident electron velocity. For this momentum the phase can be expressed as

$$\begin{aligned}
\phi &= 1/\hbar \int \frac{1}{2} m \left( \frac{-e\vec{A}}{m} + \dot{\vec{x}}_0 \right)^2 dt + e/\hbar \int \vec{A}\cdot\left( \frac{-e\vec{A}}{m} + \dot{\vec{x}}_0 \right) dt \\
&= -1/\hbar \int \frac{e^2 \vec{A}^2}{2m} dt + 1/\hbar \int \tfrac{1}{2} m \dot{\vec{x}}_0^2\, dt \\
&= -1/\hbar \frac{e^2 \vec{A}_0^2}{4m} T + C,
\end{aligned} \tag{5}$$

where $T$ is the interaction time and $C$ a constant. Consequently, the phase difference between electron paths in the laser and in the vacuum (figure 1(b)) is

$$\phi_A - \phi_{A=0} = -1 \Big/ \hbar \frac{e^2 \vec{A}_0^2}{4m} T = \Delta\phi_p, \tag{6}$$

where the last equality follows from equations (2) and (4). The last equality in equation (6) is also based on the assumption that the laser pulse is much longer than the laser period, and that there is no dependence on the carrier phase envelope. This assumption is valid for laser pulses

extending over many cycles. The ponderomotive phase shift (equation (6)) is non-dispersive, i.e. independent of the electron velocity $v_e$. The non-dispersive nature is one of the defining features of the AB-effect [20] and this property is a first justification of the nomenclature 'PAB-effect'.

(c) The above cycle-averaged description, based on the ponderomotive potential, ignores the detailed electron motion in the time-dependent laser fields. The phase shift associated with the detailed motion in the laser focus can be obtained from a time-dependent path-integral approach. As before, the phase shift for an electron in an electromagnetic potential can be written as, $\phi = 1/\hbar \int L \, dt$. Using the Hamiltonian, $H = \dot{\vec{x}} \cdot \frac{\partial L}{\partial \dot{\vec{x}}} - L$, the phase shift can be rewritten as, $\phi = \frac{1}{\hbar} \int \vec{p} \cdot d\vec{x} - \frac{1}{\hbar} \int H \, dt$, where the second term is a constant for systems (such as considered here), where the sum of the kinetic and potential energy is conserved. The same momentum as before, $m_e \dot{\vec{x}} = -e\vec{A} + m_e \dot{\vec{x}}_0$, yields the phase for an electron in a travelling electromagnetic wave: $\phi = \frac{m_e \dot{\vec{x}}}{\hbar} \int d\vec{x}$. The interferometric phase shift is thus $\Delta\phi_s = \frac{m_e \dot{\vec{x}}}{\hbar} (\int d\vec{x}_{\vec{A}} - \int d\vec{x}_{\vec{A}=0})$, where $\int d\vec{x}_{\vec{A}}$ and $\int d\vec{x}_{\vec{A}=0}$ are the path lengths (per laser period) of the electron in the presence and absence of the laser field, respectively. The motion of the electron is well approximated by

$$x(t) = \frac{eE_0}{m_e \omega^2} \sin(\omega t); \quad y(t) = v_0 t, \tag{7}$$

for an electric field propagating in the $+z$-direction, a laser polarization in the $x$-direction, and the electron is propagating in the $+y$-direction with a speed $v_0$ (see figure 1). Analytic integration of the electron path gives

$$\Delta\phi_s = \frac{m_e \dot{\vec{x}}}{\hbar} \left( \int d\vec{x}_{\vec{A}} - \int d\vec{x}_{\vec{A}=0} \right) = \frac{m_e v_0}{\hbar} \frac{\pi e^2 E_0^2}{2 v_0 m_e^2 \omega^3}. \tag{8}$$

The laser intensity is chosen low enough so that the velocity $v_0$ greatly exceeds the laser-induced velocity $eE_0/m_e\omega$. The result is that the time averaged PAB-phase shift (equations (4) and (6)) matches the time-dependent path-integral phase shift (equation (8)) $\Delta\phi_s = \Delta\phi_P$. This equality justifies at a deeper level the use of the simple ponderomotive picture.

Both the time-independent and the time-dependent path-integral approaches and the ponderomotive approach, result in the same non-dispersive phase shift. This leads us to the observation that the PAB-effect shares the non-dispersive nature of the traditional AB-effects [20]. The presence of the local interaction of the electron with the electromagnetic laser field is an indication that this is a type-II AB-effect.

(d) All the above arguments are based on the plane wave description of the laser beam. To test the validity of the plane wave approximation and investigate the detailed dynamics of the electron while in a more realistically described laser focus [26], the classical equations of motion were numerically integrated. This also allows us to check the additional requirement that the local interaction is masked by the uncertainty principle [5]. An additional benefit of the numerical analysis is the possibility to establish the absence of time delays or deflections due to forces. This property cannot be inferred from the dispersionless nature of the effect, as Peshkin [27] has shown by a counter example to the inverse of the Zeilinger theorem [28].

The numerical integration included solutions for the $\vec{E}$ and $\vec{B}$ fields valid for laser foci on the order of the wavelength of the light [26]. The laser parameters are: $\lambda = 800$ nm, $w_0 = 5\,\mu$m, $I_0 = 10^{13}$ W cm$^{-2}$, and a laser pulse length of $t_p = 15$ fs. These laser parameters correspond to readily available high-repetition rate lasers. An example electron trajectory in the femtosecond laser pulse is given in figure 2. For the chosen parameters the forces in the propagation direction

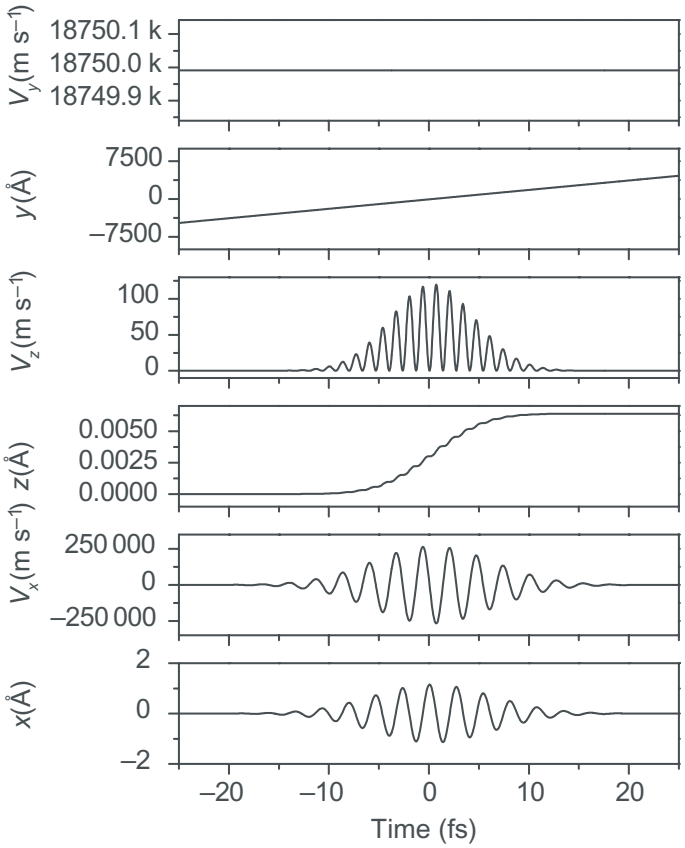


**Figure 2.** Electron trajectory in laser focus. The graphs show the numerical results for the electron trajectory when a 1000 eV electron interacts with a 800 nm, 15 fs, laser pulse with a waist of 5 $\mu$m and an intensity of $10^{13}$ W cm$^{-2}$. For each coordinate, the position of the electron along with the associated velocity is plotted versus time. In the electron propagation direction ($+y$) the electron velocity is unaffected.

are negligible compared with the forces perpendicular to the propagation direction, which justifies the earlier use of the plane wave approximation for the focus. The PAB-phase shifts from the numerically integrated path give the same phase shift as the use of approaches (a), (b) and (c).

It is also interesting to note that although the electron velocity has not changed after the laser pulse has passed, the electron trajectory does suffer a minute displacement in the $z$-direction (figure 2). Formally, this could lead to an observable. However, the displacement is much smaller than the transverse coherence length of any electron interferometer, and is thus 'protected' from observation by the uncertainty principle. Moreover, the displacement can be undone by using a second identical, but counter-propagating laser pulse in a 'Quadra-pulse' configuration [5].

Some remarks on the feasibility of a PAB experiment may also be in order. The laser beam waist must be smaller than the separation between the electron beams. For a beam separation of about 100 $\mu$m such as reached in Mollenstedt and Bayh's experiment [29] this condition is

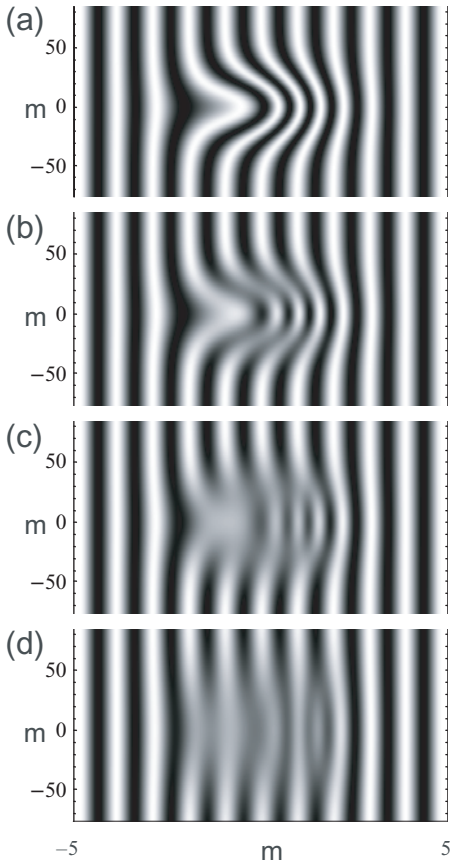


**Figure 3.** Electron interferogram for the PAB-effect. All patterns are for 1000 eV electrons, interacting with a 15 fs laser pulse with a peak intensity of $I_0 = 10^{13}$ W cm$^{-2}$. (a) A 10 fs electron pulse; (b) a 50 fs electron pulse; (c) a 100 fs electron pulse and (d) a 200 fs electron pulse.

satisfied. On the other hand, the electron beam must be much narrower than the beam waist to minimize deflection of the electrons from the slope of the ponderomotive potential. With electron collimation slits of 100 nm such as realized by Barwick *et al* [30], this is possible. The magnitude of the ponderomotive deflection is about $10^{-5}$–$10^{-4}$ rad [21]. This is small compared with the angle between the two electron beams ($\sim 10^{-3}$ rad) and the PAB-effect dominates for such an arrangement the ponderomotive deflection.

To visualize the PAB-effect in an electron interferogram, we use the following cycle-averaged intensity in equation (2),

$$I(x, y, z, t) = \frac{I_0}{\left(1 + (2z/kw_0^2)^2\right)} \times \exp\left(\frac{-2(x^2 + y^2)}{w_0^2\left(1 + (2z/kw_0^2)^2\right)} - \frac{-2(t - z/c)^2}{t_p^2}\right). \tag{9}$$

If the substitution of $y = v_0 t$ is made, then the phase shift for an electron wave can be found using equation (3). This altered electron wave front can be recombined with a plane wave to obtain an interferogram (see figure 3(a)). This pattern is a measurable signature of the PAB-effect. An example of a similar electron interferogram was obtained and used to measure

decoherence in an electron interferometer [31], which indicates the feasibility of this type of measurement.

The PAB-effect can also be used to characterize ultrashort electron pulses (<100 fs). One problem that must be overcome before electron pulse durations can be delivered on a target in the 10 fs regime is dispersion. Dispersion in electron pulses is a direct result of the energy spread inherent to all electron sources. For example, a field emission electron source triggered with a femtosecond laser [7, 8], may lead to electron pulse emission times of less than 10 fs. However, an energy spread of 0.5 eV (typical for a field emission tip) at a tip voltage of 1000 eV, leads to a temporal broadening exceeding 500 fs after the pulse has travelled 5 cm. To deliver a sub-100 fs electron pulse on a target, dispersion control must be attained along with a method to characterize the ultrashort pulse. Some methods of dispersion control are described in [10]. In figures 3(a)–(d), the interference fringes in an electron interferogram are shown for different electron pulse durations. By imaging the electron interference pattern the electron pulse dispersion can be minimized in real time.

## Acknowledgment

This material is based upon work supported by the National Science Foundation under grant no. 0653182.

## References

[1] Aharonov Y and Bohm D 1959 *Phys. Rev.* **115** 485
[2] Chambers R G 1960 *Phys. Rev. Lett.* **5** 3
[3] Tonomura A *et al* 1986 *Phys. Rev. Lett.* **56** 792–5
[4] Lee W-T *et al* 1998 *Phys. Rev. Lett.* **80** 3165
[5] Aharonov Y 1983 *Proc. Int. Symp. Foundations of Quantum Mechanics* ed S Kamefuchi (Tokyo: Physical Society of Japan) p 10
[6] Matteucci G and Pozzi G 1985 *Phys. Rev. Lett.* **54** 2469
[7] Barwick B *et al* 2007 *New J. Phys.* **9** 142
[8] Hommelhoff P *et al* 2006 *Phys. Rev. Lett.* **96** 077401
[9] Fill E *et al* 2006 *New J. Phys.* **8** 272
[10] Baum P and Zewail A H 2006 *Proc. Natl Acad. Sci. USA* **103** 16105
[11] Irvine S E, Dechant A and Elezzabi A Y 2004 *Phys. Rev. Lett.* **93** 184801
[12] Lobastov V A, Srinivasan R and Zewail A H 2005 *Proc. Natl Acad. Sci. USA* **102** 7069
[13] Gallant P *et al* 2000 *Rev. Sci. Instrum.* **71** 3627
[14] Siwick B J *et al* 2005 *Opt. Lett.* **30** 1057
[15] Hebeisen C T *et al* 2006 *Opt. Lett.* **31** 3517
[16] Irvine S E and Elezzabi A Y 2006 *Opt. Express* **14** 4115
[17] Reckenthaeler P *et al* 2008 *Phys. Rev.* A **77** 042902
[18] Hasselbach F 1988 *Z. Phys.* B **71** 443
[19] Gronniger G, Barwick B and Batelaan H 2006 *New J. Phys.* **8** 224
[20] Badurek G *et al* 1993 *Phys. Rev. Lett.* **71** 307
[21] Batelaan H 2007 *Rev. Mod. Phys.* **79** 929
[22] Dawson J F and Fried Z 1967 *Phys. Rev. Lett.* **19** 467
[23] Hsiang J-T and Ford L H 2004 *Phys. Rev. Lett.* **92** 250402

[24] Evans M W 1994 *Found. Phys. Lett.* **7** 467
[25] Jackson J D 1999 *Classical Electrodynamic* (New York: Wiley)
[26] Salamin Y I and Keitel C H 2002 *Phys. Rev. Lett.* **88** 095005
[27] Peshkin M 1999 *Found. Phys.* **29** 481
[28] Zeilinger A 1985 *Fundamental Aspects of Quantum Theory, NATO ASI Ser. B* vol 144 ed V Gorini and A Frigerio (New York: Plenum)
[29] Möllenstedt G and Bayh W 1962 *Phys. Blätt.* **18** 299
[30] Barwick B *et al* 2006 *J. Appl. Phys.* **100** 074322
[31] Sonnentag P and Hasselbach F 2007 *Phys. Rev. Lett.* **98** 200402